Published in final edited form as:
Nanomedicine (Lond). 2008 October ; 3(5): 703–717. doi:10.2217/17435889.3.5.703.

Clearance Properties of Nano-sized Particles and Molecules as Imaging Agents: Considerations and Caveats

Michelle Longmire, **Peter L. Choyke, M.D.**, and **Hisataka Kobayashi, M.D., Ph.D.***
Molecular Imaging Program, National Cancer Institute, National Institutes of Health, Building 10, Room 1B40, Bethesda, Maryland, USA. 20892-1088

Summary

Nanoparticles possess enormous potential as diagnostic imaging agents and hold promise for the development of multimodality agents with both imaging and therapeutic capabilities. Yet, some of the most promising nanoparticles demonstrate prolonged tissue retention and contain heavy metals. This presents serious concerns for toxicity. The creation of nanoparticles with optimal clearance characteristics will minimize toxicity risks by reducing the duration of exposure to these agents. Given that many nanoparticles possess easily modifiable surface and interior chemistry, if nanoparticle characteristics associated with optimal clearance from the body were well established, it would be feasible to design and create agents with more favorable clearance properties. This paper presents a thorough discussion of the physiologic aspects of nanoparticle clearance, focusing on renal mechanisms, as well as provides an overview of current research investigating clearance of specific types of nanoparticles and nano-sized macromolecules, including dendrimers, quantum dots, liposomes and carbon, gold, and silica-based nanoparticles.

Keywords

nanotechnology; nano-materials; nanoparticles; macromolecules; clearance; excretion; kidney; molecular imaging; liver; toxicity

Introduction

Nanoparticles and nano-sized molecules possess enormous potential as diagnostic imaging agents and hold promise for the development of multimodality agents with both imaging and therapeutic capabilities. Generally defined as molecules with lengths that range from 1 to 100 nm in at least 2 dimensions, nanoparticles and nano-sized molecules show remarkable structural diversity and include nano-tubes, dots, wires, fibers, and capsules [1]. Although nanotechnology has exciting implications for medicine, this technology presents challenges regarding particle biocompatibility and much is to be learned regarding the understanding of small particle behavior *in vivo*. Unlike conventional imaging agents and therapeutics, many nanoparticles are highly stable *in vivo*—exemplified by a recent study suggested that quantum dots may be retained in the body (and remain fluorescent) for more than 100 days [2]. Additionally, some of the most promising nanoparticles currently under investigation contain heavy metals, which not only pose a risk for toxicity, but prolonged particle retention may interfere with diagnostic testing and imaging [3].

*Address Correspondence to: Hisataka Kobayashi, M.D., Ph.D. Chief, Preclinical development Section, Molecular Imaging Program, NCI/NIH Building 10, Room 1B40, MSC 1088 Bethesda, Maryland, USA 20892-1088 Ph 301-435-4086; Fax 301-402-3191; kobayash@mail.nih.gov.

Creating particles with optimal clearance characteristics will minimize toxicity risks and decrease concerns of nanoparticle and nano-sized molecules interference by reducing the duration of exposure to these agents. Given that many types of nanoparticles possess easily modifiable surface chemistry, if nanoparticle characteristics associated with optimal clearance were well established, it would be feasible to create agents with more favorable clearance properties. Properties currently known to affect clearance include particle material, size, shape, surface chemistry and charge—all of which vary depending on the individual particle type and modifications made for specific applications. This paper presents a thorough discussion of the physiologic aspects of nanoparticle clearance, focusing on renal mechanisms, as well as provides an overview of current research investigating clearance of specific types of nanoparticles and nano-sized molecules, including dendrimers, quantum dots, liposomes and carbon, gold, and silica-based nanoparticles.

Physiologic Considerations

Vascular Delivery

Upon intravenous administration, nanoparticles (NPs) and nano-sized molecules (NMs) enter the vascular system and are distributed to the organs and peripheral tissues of the body. Within the vascular compartment NPs encounter blood cells, platelets, coagulation factors, and plasma proteins and depending on the size and charge, NPs and NMs may undergo adsorption or opsonization by serum proteins. In addition to enhancing particle recognition by the host immune system, adsorption/opsonization of NPs alters the effective size of the particle and results in a particle diameter referred to as the *in vivo* hydrodynamic diameter (HD)—which may be considerably larger than the *in vitro* diameter of the NP. The HD affects blood clearance and therefore blood half-life and whole body half-life. The HD is inversely related to rate of glomerular filtration and is directly related to blood and whole body half-life.

The vascular endothelial cell monolayer acts as a dynamic, semiselective barrier that regulates transport of fluid and macromolecules between the vascular compartment and the extravascular space [4]. Although the structure of the endothelial layer varies throughout the body, the effective pore size in normal intact endothelium is about 5 nm [3]. Nano-sized molecules with an HD less than 5 nm achieve rapid equilibrium with the extravascular extracellular space (EES), whereas larger particles experience prolonged circulatory times due to slow transport across the endothelium. For example, when administered intravenously human IgG (HD:11 nm) requires 24 h to equilibrate between the vascular compartment and the EES [3,5,6]. In contrast, smaller molecules such as the radiocolloid dextran-Technetium 99 (HD: < 4 nm), establish rapid equilibration with the EES due to penetration of capillary fenestrae [7]. Similar behavior has been observed in the lymphatic vessels with NPs. Although the lymphatic vessel endothelial layer is more permeable than that of the vascular endothelium because of its role in clearance of macromolecules from the EES, particles up to or smaller than 6 nm in diameter can flow easily into and out of the lymphatic vessels [8]. Therefore, the threshold of nano-size diffusion from the lymphatics is slightly larger than the capillaries but still comparable.

Modification of NP/NM characteristics such as size and surface chemistry can significantly alter *in vivo* kinetic properties of NPs and NMs. PEGylation, the process of molecularly attaching polyethylene glycols (PEG) with different molecular weights to the particle surface groups, is one of the most widely used methods for improving particle pharmacokinetic behavior [9]. The primary effects of PEGylation include changes to plasma half-life of the agent, tissue distribution, and particle elimination [9].

Renal Clearance

The kidney is capable of rapidly removing molecules from the vascular compartment mostly as the injected forms and therefore, renal excretion represents a desirable pathway for NP removal with minimal catabolism or breakdown from the human body to avoid the possible side effects. Therefore, in this review, we are focusing mainly on the renal clearance. Renal clearance of intravascular agents is a multifaceted process involving glomerular filtration, tubular secretion, and finally elimination of the molecule through urinary excretion. As intravascular agents enter the glomerular capillary bed, molecules are either filtered through the glomerular capillary wall and into the proximal tubule, or remain within the vascular compartment (Figures 1 and 2). The glomerular capillary wall is composed of three layers: fenestrated endothelium; glomerular basement membrane (GBM); and the foot processes of glomerular epithelial cells, which are separated by filtration slits bridged by slit diaphragms [10]. It is generally accepted that glomerular filtrate flows through the fenestrate, across the GBM, and through the filtration slits [10]. Among the key nanostructural dimensions is the slit diaphragm, which is approximately 43 nm in diameter [10]. However, after taking into considering the combined effects of each layer of the glomerular capillary wall, the functional or physiologic pore size is significantly smaller—measuring only 4.5-5 nm in diameter [11].

Filtration of particles through the glomerular capillary wall—glomerular filtration—is highly dependent on molecule size and is referred to as the filtration-size threshold [10]. Molecules with an HD < 6 nm are typically filtered, while those > 8 nm are not typically capable of glomerular filtration. Filtration of molecules within the intermediate range, 6-8 nm in HD, depends upon both size and charge of the particle. The filtration-size threshold for globular proteins has been well studied and is generally accepted to be < 5 nm in HD. For example, inulin (HD: 3 nm) achieves 100% renal filtration with a blood half life of only 9 minutes [12]. The relationship between protein size and clearance is further demonstrated by antibody clearance data. The stabilized V region fragment of an antibody protein (HD: 4 nm) achieves 100% renal filtration with a serum half life of 5 minutes [13] as compared to the antibody Fab' fragment (HD: 6.0 nm) which achieves only 9% effective filtration into the urine with a serum half-life of 28 minutes [5,14]. Additionally, clearance of antibody fragments is more rapid that that of the full intact antibody, which is not efficiently filtered and has a serum half-life up to many days.

Although the fate of globular proteins in the kidney provides an important framework for understanding general properties of renal clearance, the physical properties of NPs differ from those of proteins in several ways. NP shape, surface chemistry, and interior charge is distinct and unlike proteins, which are heterogeneous and polydispersive, NPs can be synthesized with near-spherical shape and identical surface chemistry [15]. Such differences may lead to distinct renal handling of NPs compared to protein molecules. To evaluate the effect of these characteristics on filtration-size threshold, clearance studies of PAMAM dendrimer-based NPs with homogenous chemical properties and near-spherical shape were conducted. Results showed that PAMAM dendrimers < 6 generations or about 5.4 nm in diameter demonstrated effective glomerular filtration [16,17] (Figure 3). This filtration-size threshold is similar to that of conventional molecules. Additionally, renal clearance studies in mice using quantum dots revealed that renal excretion was observed for dots with HDs ranging form 4.36-5.52 nm [3]. Quantum dots > 8 nm (HD = 8.65 nm) did not demonstrate renal filtration but instead exhibited uptake in the reticuloendothelial system (RES) and lung [3]. The relationship between HD, renal clearance, and total body retention was determined to be sigmoidal with the 50% point for total body clearance at 4 h achieved with an HD of 5.5 nm [3]. Results of this study also suggests that the filtration-size threshold for of NPs may comparable to proteins and other nano-sized molecules. With these data in mind it is reasonable to conclude that NPs capable of being synthesized < 8 nm in diameter, such as

dendrimers, fullerenes, carbon nanotubes, silica particles and quantum dots, can undergo renal clearance if other modifiable parameters (surface charge and chemistry) are optimized for this excretion pathway.

In addition to size, surface charge is also an important determinant of the renal handling of nano-sized molecules. The effect of molecular charge on renal filtration is due to at least 2 factors: 1) potential interactions between charged molecules and serum proteins, resulting in increased HD due to particle adsorption [3], and 2) interactions between charged molecules and fixed charges within the glomerular capillary wall [10]. Studies using quantum dots as a model for *in vivo* NP clearance revealed that purely anionic or cationic charge was associated with agent adsorption by serum proteins [3]. Adsorption resulted in an increase in the HD to > 15 nm, dramatically reducing renal filterability [3]. Neutralization of the NP surface via PEGylation was shown to be effective in preventing serum protein adsorption; however, it was reported that synthesizing a PEGylated QD with an HD < 10 nm was not possible [3]. Therefore, PEGylation, also dramatically reduces particle renal filtration [3]. Interestingly, zwitterionic coatings were shown to prevent serum protein adsorption and were associated with the highest solubility and smallest HD [3].

Studies evaluating the effect of molecular charge on glomerular filtration of similarly sized molecules have shown that filtration is greatest for cationic molecules, followed by neutral molecules, while anionic molecules are least readily filtered through the glomerular capillary wall (Figure 2) [10,11]. Direct comparison of differently charged molecules with respect to their glomerular filtration has been studied using a charge-modified Fab (HD: 6 nm), which was created by blocking branching amine residues with glycolate [18]. Weakly anionic Fab showed drastically less filtration compared to weakly cationic Fab fragments [18]. Charge-selective filtration is attributed to fixed negative charges within the capillary wall [10]. Molecular charge is of particular significance for the filtration of molecules within the 6-8 nm range, as these particles are not small enough to undergo charge-independent filtration, yet may still be filtered if molecular charge is favorable.

The final step in renal processing occurs at the proximal tubule where filtered molecules may be resorbed from the tubular fluid and previously unfiltered molecules may be actively secreted into proximal tubule lumen. Particle behavior at the proximal tubule is an important consideration because some molecules, such as glucose, achieve 100% resorption, negating the effects of glomerular filtration, while other agents, such as heavy metals, are highly toxic to proximal tubule cells and may potentially cause renal damage including acute tubule necrosis, interstitial nephritis and even renal failure. Research evaluating NP/NM reabsorption at the proximal tubule is currently limited. Studies by Kobayashi et al indicate that some polyamine dendrimers may undergo proximal tubule reabsorption [Kobayashi, 2004 #81], but further investigation of this issue is needed to gain insight into the renal toxicity profile of nano-sized particles. Evaluation of agent behavior at each step in renal processing may lead to agents with optimal biocompatibility and clearance properties.

Hepatic Clearance

The hepatobiliary system represents the primary route of excretion for particles that do not undergo renal clearance. The liver provides the critical function of catabolism and biliary excretion of blood-borne particles as well as serves as an important site for the elimination of foreign substances and particles through phagocytosis [19]. All NPs and NMs, which are excreted via the biliary system, are catabolized first through hepatocytes. All physical or chemical catabolites must be accounted for when considering total hepatic clearance. Therefore, the hepatic clearance is more complex than renal clearance. Phagocytic Kupffer cells have ciliated borders and stellate branches that serve as highly adapted mechanical traps for the removal of unwanted substances from the blood including foreign colloidal or

particulate substrates [19]. Kupffer cells possess numerous receptors for selective endocytosis of opsonized particles (receptors for complement proteins and for the Fc part of IgG) and are the primary site for iron transport and metabolism [19]. Hepatocytes also play an important role in liver clearance through endocytosis and enzymatic breakdown of foreign particles. Although the phagocytic capacity of hepatocytes is much less than that of Kupffer cells, these cells represent an important physiologic pathway for foreign particle processing and are a potential site for toxicity [19]. An important difference exists, however, between hepatocytes and Kupffer cells. Hepatocytes are within the pathway for biliary excretion and therefore particles processed by these cells are potentially excreted into the bile. Kupffer cells are part of the RES and rely exclusively on intracellular degradation for particle removal. Similar to all phagocytic cells of the RES, particles that are not broken down by intracellular processes will remain within the cell and will therefore be retained by the body.

One of the physiologic functions of the liver is to efficiently capture and eliminate particles on the scale of 10-20 nm for the clearance of viruses and other small particles [3]. As a result of this adaptation, agents within this size range often undergo rapid liver uptake [3]. To achieve adequate retention times, nanoparticles may require modification to prevent or lessen opsonization. Molecular modification via PEGylation is a widely used mechanism to decrease first-pass extraction and increase NP serum half-life. Interestingly, although uptake of particles from the blood to the liver may occur relatively quickly, hepatic processing and biliary excretion of these particles is relatively slow, often resulting in prolonged retention of NPs within the liver parenchyma itself [3].

Nanoparticle Composition and Clearance

Each class of NP possesses a distinct chemical composition and possible range of sizes (Figure 4). The characteristic properties of each distinct type of nanoparticle influence pharamacokinetics and demonstrate that size is not the only determinant of *in vivo* behavior. Next we discuss current research regarding the clearance of the various types of widely used nano-sized particles with emphasis on molecules < 100 nm. Therefore, we did not include some types of large NPs including nano-bubbles, emulsions, etc. because these NPs only be cleared through the liver or RES.

Dendrimers

Macromolecular contrast agents were first developed for MR angiography (MRA) due to the inability of conventional low molecular weight gadolinium (Gd)-(III) agents to provide vessel opacification times adequate to permit MR imaging. Compared to conventional agents, which demonstrate rapid equilibration with the EES and are quickly cleared by renal filtration, macromolecular agents demonstrate prolonged vascular retention times, a trait that was previously necessary for MR imaging [20]. Among the macromolecular agents, dendrimers are a class of highly branched synthetic spherical polymers [15,21,22]. Two commercially available types of dendrimers have been investigated well as imaging agents, one type within the poly(propyleneime) (PPI) dendrimer series, consisting of a 1,4-diaminobutane (DAB) core, and the other of the poly(amidoamine) (PAMAM) dendrimer series possessing a 1,2-diaminoethane core. The defined structures and availability of the surface amino groups of dendrimers has led to the development of dendrimer-conjugates with a variety of chelates for use as MR contrast agents [15,24].

Given the small size of dendrimer NPs, 3-10 nm, it is not surprising that dynamic imaging studies of dendrimer-based MR contrast agents (PAMAM-Gd-(III) conjugates) revealed that renal excretion was the major route of clearance for dendrimer NPs functionalized with Gd (III) and that renal clearance of dendrimer-based MR contrast agents was size dependent

[25,26]. Studies comparing clearance of dendrimers with DAB and PAMAM cores have shown that renal clearance of DAB-based agents was more rapid than that of PAMAM-based agents of the same dendrimer generation [27]. However, greater than 60% of the injected doses of the DAB-G3-, DAB-G2-, or PAMAM-G2-based contrast agents was shown to be cleared from the body within 15 min after injection [27].

Although renal clearance has been shown to be the primary route of excretion for both DAB and PAMAM dendrimers, when directly compated, DAB dendrimers demonstrated greater liver accumulation compared to the same generation PAMAM-based NP [27]. However, DAB-based agents demonstrated higher signal intensities than PAMAM agents in the kidney, possibly indicating that these agents were retained within the kidney [27]. Interestingly, despite greater liver accumulation, DAB-G4 have been shown to be excreted from the body faster than PAMAM-G4, indicating rapid hepatic uptake and excretion [27] probably because the shorter interior structure of propylimine (PI) makes entire structure physically smaller.

Gadomer-17 (Schering AG, Berlin, Germany) is a newer dendrimer, large enough to prevent extensive leakage into the EES, yet, small enough to undergo effective renal clearance [28,29]. Studies examining clearance of Gadomer-17 indicate that the agent is cleared via glomerular filtration with a terminal phase half-life of 10 minutes in rabbits [29].

Inorganic biodegradable co-polymers

Clinical use of Gd-containing macromolecular agents has been limited by safety concerns for the potential of prolonged exposure to free-unchelated Gd-(III). Clinically approved low-molecular-weight contrast agents undergo more rapid elimination via renal filtration compared to macromolecular agents. As a result, toxicity due to free Gd-(III) by conventional agents has been considered to be negligible with the exception of patients in renal failure, in whom tissue retention is possible [28]. Biodegradeable Gd-(III) containing NPs have been developed to address the need for a contrast agent with clearance characteristics similar to low-molecular-weight agents yet possessing vascular retention characteristics comparable to macromolecular agents [30].

In vivo, biodegradable agents initially behave as macromolecular agents for blood-pool imaging and then degrade to low-molecular weight complexes that are rapidly excreted by the kidney [30]. Biodegradable contrast agents consist of polydisulfide Gd-(III) complexes [31] and *in vivo* these disulfide bonds are readily degraded into smaller Gd(III) complexes by endogenous thiols—including glutathione, cysteine, and homocysteine—via disulfide-thiol exchange reaction [30-32]. The resulting smaller units are then cleared through renal filtration [28,30,32]. Currently, biodegradable agents include Gd-DTPA cystamine copolymers (GDCC), Gd-DTPA cystine copolymers (GDCP) and Gd-DTPA cystine, diethyl ester copolymers (GDCEP) and each has been shown to demonstrate slightly different biodegradability [30,32].

Pharmacokinetic studies comparing the anionic agent, GDCP, and the neutral agent, GDCEP, to a similar nonbiodegradable macromolecular agent revealed that both GDCP and GDCEP cleared more rapidly from the vascular compartment and the body than the nonbiodegradable agent. This implies that degradation of the polydisulfide Gd-(III) complexes begins immediately upon intravenous injection and that smaller Gd-(III) complexes are rapidly excreted through renal filtration [30]. Neither of the biodegradable agents demonstrated significant accumulation in bone, heart, or lung, but interestingly, much higher accumulation was observed in the liver and spleen with the anionic GDCP than with the GDCEP particle [30]. This may be due to decreased renal filtration of the anionic form.

Quantum Dots

Quantum dots (QD) represent an emerging new class of probes for *in vivo* fluorescence imaging. These semiconductor nanocrystals are capable of size-tunable light emission, demonstrate superior brightness to organic dyes and fluorescent proteins, are resistant to photobleaching, and have broad absorption spectra, which permits simultaneous excitation of multi-color QDs with a single excitation source. Structurally, quantum dots possess a core/shell architecture 2-8 nm in diameter with the size adjusted for the wavelength of fluorescence emission desired [33]. However, QD size can increase dramatically, depending on the coating layer surrounding the core. Currently there is considerable excitement regarding the development of QDs for medical applications, however, since many contain heavy metals such as cadmium and selenium, rapid clearance will likely be a prerequisite to clinical use. Additionally, although plasma half-lives of QDs may be short, QD retention within organs is another issue. Intravenously injected QDs have been shown to be detectable in liver and kidney 28 days post injection [34] and within the lymph nodes and bone marrow of mice 133 days after injection [35,36].

Studies examining the renal clearance of QDs have been recently been conducted as Choi et al. defined the relationship between hydrodynamic diameter, renal clearance and total body retention for quantum dots of difference sizes. The 50% point for total body clearance of quantum dots at 4 h was determined to be an HD of approximately 5.5 nm. Serum half-life of particles ranging from 4.36-8.65 nm was shown to correlate positively with size, ranging from 48 min to 20 h. Data demonstrated that renal clearance was the primary excretion route for dots with HD ranging from 4.36-5.52 nm with renal clearance decreasing with increasing size. Larger quantum dots did not demonstrate renal clearance and instead accumulated in the liver, lung, and spleen.

Choi et al also demonstrated that charge affected the renal clearance of QDs. Due to charge-related adsorption by serum proteins, purely anionic or cationic charge increased hydrodynamic diameter to > 15 nm. This increase in size significantly decreased the renal clearance of these particles and likely shifted the route of excretion from the kidney to the liver. Interestingly, zwitterionic coatings prevented serum protein adsorption—resulting in improved renal filtration. Zwitterionic particles also had the highest solubility and smallest hydrodynamic diameter. This data suggests that creating particles with zwitterionic surface charges may be a useful approach to obtaining more favorable clearance properties in QDs intended for clinical applications.

In addition to the kidney, the liver also has an important role in the clearance of bio-conjugated or larger (> 8 nm) QDs. Fischer et al examined clearance of QDs is rats and found that bovine serum albumin (BSA) conjugated to an organic coated QD hastened clearance (0.59 +/− 0.16 mL min(−1) kg(−1) for unconjugated compared to 1.23 +/− 0.22 mL min(−1) kg(−1) for BSA conjugated) and resulted in significantly higher levels of liver uptake [37]. Additionally, Schipper et al evaluated the clearance of commercially available CdSe QDs of two sizes, 12 nm and 21 nm, and evaluated the effect of pegylation on clearance. Both sizes demonstrated rapid uptake by the liver although pegylation was associated with slightly slower uptake [38].

Carbon Nanoparticles

There is great interest regarding the use of carbon nanostructures such as C_{60} fullerenes and nanotubes in medical therapeutics and imaging. Carbon nanostructures such as C_{60} fullerenes and shortened single-walled carbon nanotubes (SWNTs) have already demonstrated considerable promise as contrast agents. Positive characteristics of these particles include improved relaxivity compared to conventional contrast agents (when

loaded with Gd-(III)), an outer carbon sheath that is easily functionalized for targeting, a good track record of biocompatibility, and favorable lipophilicity and size for crossing cell membranes for intracellular accumulation, since particles as small 1 nm can be synthesized [39].

Within the field of MR imaging, Gd-(III)-containing metalofullerenes, or gadofullerenes, show potential as a new generation of higher-performance contrast agents [40-44]. Confinement of the Gd-(III) within the fullerence cage prevents dissociation of toxic Gd ions *in vivo*, therefore decreasing risk of toxicity [40]. In addition, specifically derivatized Gd C_{60} nanoscale materials, with diameters of only 1nm, have been shown to have 20 times the relaxivity of conventional MR imaging agents [40,44]. However, clinical implementation of these compounds has been limited by their demonstrated RES accumulation as well as by problems with spontaneous aggregation *in vivo* (observed with polyhydoxylated fullerene derivatives) [45]. With these issues in mind, water-soluble formulations that demonstrate renal excretion have recently been developed [42]. Studies evaluating *in vivo* behavior of water-soluble Gd C_{60} 60derivative, {Gd C60[C(COOH)2]10} gadofullerenes, have shown that these agents demonstrate decreased RES uptake and increased urinary excretion [42]. In these studies, particles were quickly detected in the kidney and exhibited excretion via the bladder within 1 hr of injection [42]. The development of a fullerene MR contrast agent excreted by the kidney represents an important step in the development of clinically feasible carbon nanostructure-based contrast agents [42].

Single-walled carbon nanotubes (SWNTs) are also emerging as an important class of nanomaterials for molecular imaging. Due to their relative ease of synthesis compared to metallofullerenes and the substantially greater relaxivity achieved by gadolinium-based SWNT contrast agents compared to conventional contrast agents, SWNT-based contrast agents will likely be an important development for MR imaging [39]. In addition, their intrinsic near-infrared fluorescence makes SWNTs a promising optical agent as well [46]. SWNTs also have distinct Raman Spectroscopy signatures enabling their detection with yet another type of detector. However, clinical implementation of SWNTs requires overcoming the RES uptake associated with the lipophilicity of purely carbon NPs.

In vivo behavior of intravenously injected carbon nanotubes has been studied using radiolabeling, isotope-ratio mass spectroscopy methods, and Raman scattering [46-48]. Singh *et al* evaluated the clearance of an intravenously administered water-soluble carbon nanotube radiotracer consisting of a chemically functionalized SWNT covalently linked to ^{111}Indium [47]. Gamma scintigraphy data revealed that functionalized SWNTs demonstrated rapid removal from the systemic circulation through renal clearance [47]. The particle half-life was found to be 3 h without any agent retention in the RES [47]. In addition, urine excretion studies have revealed that both functionalized SWNTs and multiwalled nanotubes are excreted as intact nanotubes [47]. It is noteworthy that clearance studies involving pristine single-walled carbon nanotubes have shown significant RES tropism and liver accumulation of these particles (attributed to the lipophilicity of the carbon atoms), while chemically functionalized SWNTs have demonstrated renal clearance with insignificant RES uptake [46]. Further clearance studies are needed to assess the influence of chemical functionalization on SWNTs tissue tropism and clearance.

Liposomes

Liposome-based nanoparticles have been successfully used for the delivery of anti-cancer drugs, enzymes, proteins, and imaging contrast agents. There are three classes of liposomes: unilamellar vesicles of 25 – 50 nm in size, large unilamellar vesicles and multi-lamellar vesicles consisting of several lipid layers separated by aqueous fluid [49,50]. Liposomal

clearance has been shown to be governed by vesicle opsonization by serum proteins and subsequent uptake by the RES [51]. As a result factors affecting liposome opsonization including, particle charge, size, and membrane composition, are important determinants in liposome clearance [51].

Evidence indicates that serum protein opsonization of liposomes directs vesicles towards phagocytosis by cells of the RES [51]. It is thought that serum complement protein attachment to the liposomal surface during circulation leads to efficient clearance by phagocytic cells [51]. Studies have shown an inverse relationship between serum protein binding and clearance time, as liposomes with more extensive serum protein interactions are cleared more rapidly from the circulation compared to liposomes with less opsonization by serum proteins [51,52]. Among the different type of serum opsonins, the complement system has been identified as a key effector of liposome clearance [51,52]. Interestingly, both anionic and cationic liposomes have been shown to activate the complement system whereas neutral vesicles have not been shown to cause complement activation [53]. The described clearance mechanism of liposomes is likely due to complement-mediated phagocytosis by Kupffer and endothelial cells of the liver as well as other phagocytic cells of the RES [54].

In addition to opsonization, vesicle diameter and lipid composition are important determinants in liposome clearance as studies have shown that increased size was associated with more rapid clearance from circulation [51,55]. Studies suggest that the significance of size is related to the extent of opsonins bound to the liposome surface [51,55]. Larger liposomes have more extensive opsonin binding, which results in enhanced uptake via liver phagocytosis [51,56]. Liposome composition also affects vesicle clearance. Interestingly, a synergistic relationship between cholesterol content and hepatic clearance of medium (400 nm) and large (800 nm) liposomes has been established however, no relationship has been identified between cholesterol content and clearance rate for smaller vesicle sizes (*43*,[57]. Additionally, data indicates that taking into account both size and cholesterol content results in more accurate prediction of liposome clearance than either parameter alone [57].

Studies evaluating the clearance of liposomes for imaging applications specifically, have included evaluation of the pharmacokinetics and biodistribution of liposome encapsulated MR and CT agents following intravenous administration in mice [58]. Agents consisting of liposome encapsulated iohexol, a conventional iodine-based CT agent and liposome encapsulated gadoteridol, a conventional gadolinum-based MR agent, demonstrated that circulation half-lives were 18.4 ± 2.4 h and 18.1 ± 5.1 h for each agent, respectively [58]. Total plasma clearance rate was 0.00219 mL/h/g for liposomal iohexol and 0.00206 for liposomal gadoteridol [58]. Comparison of liposomal encapsulated agents to free agents revealed that liposome encapsulation significantly increased circulation half-life. Liposomal iohexol demonstrated enhanced elimination in the kidney and the spleen compared to liposomal gadoteridol [58], possibly due to known differences in clearance mechanisms of the individual contrast agents in the kidneys [59,60].

Gold Nanoparticles

Due to its inert nature, extreme resistance to oxidation, and considerable biocompatibility, gold represents an attractive metal for nanoparticle development. Metallic colloidal gold nanoparticles are widely used and are available in a variety of different forms and sizes. Recent studies have focused on the application of gold NPs as radio-opaque contrast agents, in place of the traditional iodinated molecules dissolved in liquids [61]. Additionally, gold-coated nanoshells represent promising optical imaging agents due to their tunable plasmon resonance, which enables particles to be specifically designed to match the wavelength desired for a particular application [62]. Gold nanoparticles currently in use vary in size and

include particles 1.9 nm in diameter (ultrasmall gold nanoparticles) for X-ray contrast, ≤ 40 nm in diameter for gold-gold sulfide nanoshells, and 50-500 nm in diameter for silica-gold core-shell nanoshells [61,63,64]. One notable advantage of gold NPs is that the surface charge is easily modified for more favorable excretion properties. Proteins spontaneously chemisorb to gold surfaces when incubated with metal at or slightly basic to their isoelectric point and more stable bonds can be created by utilizing the self-assembling properties of proteins with thiol/disulfide bonds onto gold surfaces to create a dense network of thiol/disulfide sulfhydryl moieties that can be easily functionalized to achieve optimal excretion surface chemistry [62].

The excretion of ultrasmall gold nanoparticles 1.9 nm in diameter developed for use as X-ray contrast agents has been studied in mice [61]. Studies demonstrated that serum gold concentration decreased in a biphasic manner, with a 50% drop between 2 min and 10 min followed by a slower decrement of another 50% between 15 min and 1.4 h [61]. In addition, the highest tissue concentration 15 min after injection was achieved in the kidney with whole body gold clearance of 77.5% of the total injected gold after 5 h [61]. These studies suggest that the kidney is the primary site for clearance of these particles.

A study conducted by De Jong et al. examined the influence of gold colloid particle size on tissue distribution in rats and revealed that size was a key determinant of *in vivo* particle distribution. The study measured end-organ particle content of spherical gold colloid nanoparticles (measuring 50, 100, and 250 nm in diameter) 24 h after intravenous injection [65]. The smallest particle studied (10 nm) demonstrated the most widespread tissue distribution at 24 h after injection. In contrast to the larger particles, the 10 nm particles were detected in all of the evaluated organs [65]. Comparison of organ particle deposition between large and small particles revealed that particle deposition for the 10 nm particle was greatest in the liver, followed by blood, spleen, kidney, lungs, brain, reproductive organs, thymus and heart; whereas the 50, 100 and 250 nm particles were only significantly deposited in the liver, spleen and blood [65]. However, the majority of the nanoparticles accumulated in the liver, irrespective of size [65]. Notably, the study did not directly evaluate clearance and did not measure urine particle losses, so kidney particle levels reflect NPs present in the kidney at the time of harvesting rather than levels that may have been cleared by the kidneys. However, the predominance of liver accumulation suggests that the hepatobiliary system was the primary site for agent clearance for NPs from 10-250 nm.

Several new gold nanoparticles have recently emerged, including gold nanocages. Currently, the smallest gold nanocage is approximately 40 nm in diameter with a wall thickness of 3.3 nm [66]. Studies examining clearance of gold nanocages are currently lacking and it is assumed that they behave similarly to conventional gold colloids; however, experimental data is needed to validate this assumption [66]. The creation of readily administrable nontoxic gold nanoparticles with optimal *in vivo* pharmacokinetic properties will have a significant effect on future advances in the development of nanoscale imaging [67]

Magnetic Nanoparticles

Magnetic nanoparticles (MNPs) are currently available as contrast agents for MRI and possess great potential for use in drug-delivery tracking. MNPs differ from traditional ferromagnetic particles in that they possess no magnetic properties outside an external magnetic field [68]. MNPs demonstrate specific-uptake by the monocyte-macrophage system, and are therefore widely evaluated MRI markers for the diagnosis of inflammatory and degenerative disorders associated with high macrophage activity [69]. Currently, there are two types of MNPs used in medical imaging: 1) superparamagnetic iron oxide (SPIO) particles with a mean HD of > 50 nm, including the feruxomides (Endorem [Guerbet Villepinte, France] or Feridex IV [Advanced Magnetics, Cambridge, MA] and 2) ultrasmall

superparamagnetic iron oxide (USPIO) particles with an HD < 50 nm, such as Ferumoxtran-10 (Advanced Magnetics, Cambridge, MA) [70].

Given intravenously, iron oxide nanoparticles are primarily cleared from the blood by the RES. The blood half-lives of the various iron oxide nanoparticles currently in clinical use vary from 1 h to 24-36 h [69]. However, specific biodistribution and clearance parameters depend on particle properties such as surface characteristics, shape, and size [71]. For example, USPIOs demonstrate biodistribution to lymph nodes in addition to the RES, whereas SPIOs do not have significant lymph node localization. [72]. Interestingly Neurberger et al. demonstrated that larger-sized MNPs are eliminated from the bloodstream faster than smaller-sized particles.

Typical MNPs have a dextran or starch coating that acts as a stabilizing agent to form a water-dispersible system [72]. It is noteworthy, however, that differences in coating chemistry impact opsonizationization with resulting effects on biodistribution and clearance [72]. Use of coating materials such as Pluronic and polyethylene glycol are known to inhibit opsonization of injected particles and may be used to selectively minimize RES uptake [72]. Pharmacokinetic studies of an iron oxide nanoparticle coated with oleic acid and Pluronic (BASF Corp., Mt. Olive, NJ) and an HD of 193 nm in rats revealed that 55% of the injected dose of iron localized in the liver compared to 75% observed with typical dextran coatings [72]. The importance of coating is further emphasized by data that has demonstrated that coating material characteristics have a more significant affect on biodistribution and blood half-life than particle size for iron oxide MNPs < 40 nm [73].

Interestingly, iron particles and coating materials may undergo different clearance mechanisms. Studies examining the clearance of the USPIO, Ferumoxtran-10 (Advanced Magnetics, Cambridge, MA), a 30 nm in diameter MNP with an iron oxide core coated with low molecular weight dextran, demonstrated that the dextran coating undergoes progressive degradation and was almost exclusively eliminated in the urine (89% in 56 days), with only a small amount excreted in the feces [74]. The iron contained in Ferumoxtran-10 was incorporated into the body iron stores and was later found in red blood cells in the form of hemoglobin [74]. Similar to endogenous iron, it was eliminated very slowly as evidenced by only 16-21% elimination after 84 days via hepatobiliary excretion (<1% urinary excretion) [74]. Similar behavior has been reported for SPIO feruxomides [74].

Intracellular metabolism plays an important role in the removal of MNPs by the liver [69]. Kupffer cells in the liver are the primary site for intracellular iron metabolism and the rate of metabolism is in part dependent on the concentration of iron oxide taken up by each cell type [72]. As a result, the rate of iron oxide metabolism in the liver is assumed to be a function of the dose injected, percent initially taken up, and the cellular distribution in the liver [72,75]. Interestingly, smaller iron oxide particles have been shown to undergo metabolism equally in hepatocytes and macrophages [Briley-Saebo, 2004 #29]. This is important since both concentration and specific distribution within the liver cells are thought to influence rate of liver metabolism [72].

Silica

New NPs are constantly emerging and the clinical viability of these agents will certainly depend on their biocompatibility and clearance characteristics. Among the newer NPs, silica is a promising material for the development of bio-compatible particles. Dye-doped silica nanoparticles are emerging optical imaging agents, ranging from a few nanometers to over 100 nm in diameter [76]. Advantages to dye-doped silica NPs include high emission intensity, excellent photostability, water solubility, and an easily modifiable surface [76]. Mesoporous silica nanospheres represent another silica-based emerging NP. Mesoporous

materials represent an ideal platform for MR-enhancing hybrid materials due to their high surface areas and tunable pore sizes [77]. Mesoporous silica NPs loaded with Gd-(III) have been developed as effective MR contrast agents [77]. The development of porous nanoparticles that allow ready access of water molecules to magnetic centers is an important step in the development of nanoparticle contrast agents for MR imaging [77]. Unfortunately, clearance studies of silica-based NPs have not yet been reported. However, such studies will provide important information regarding the behavior of these particles *in vivo* as well as provide insight into the clinical viability of silica-based particles.

Conclusion

Nanoparticles represent a promising technology for the detection and treatment of human diseases such as inflammatory conditions and cancer. Yet this field poses many new questions regarding the pharmacokinetic behavior and safety of nanometer sized particles within living systems. In standard practice, the US Food and Drug Administration requires that agents administered for diagnostic purposes be cleared completely from the human body within a reasonable time period [3]. This is a prudent approach given that the time required for total body clearance is directly related to total agent exposure. Although nanoparticles are known for their wide variability in shape, size, and chemistry, trends regarding particle clearance do seem to be generalizable despite particle differences. Given that renal filtration represents the ideal route for NP removal from the body, this review demonstrates particles may be optimized to increase renal clearance by modifications including size < 6 nm and zwitterionic or cationic surface charge [3]. Additionally, future research exploring alternative mechanisms for the removal of nanoparticles, such as by intracellular degradation may, lead to the utilization of currently unexploited pathways for particle clearance.

Clearance of metal-containing nanoparticles is an especially important consideration due to agent toxicity and potential for interference with other diagnostic imaging modalities. Metal nanoparticles may interfere with X-ray imaging due of changes in linear attenuation coefficient, magnetic resonance imaging because of proton-free voids, ultrasound because of increased echogenicity, and possibly even single photon emission computed tomography and positron emission tomography (PET) because of photon attenuation [3]. In addition, metal-containing nanoparticles require a solubilizing organic coating for biological compatibility, which increases HD and results in increased retention times [3].

Given that particle elimination continues to limit progress towards the clinical use of many of the emerging nanoparticles developed for imaging applications, a comprehensive understanding of the basic determinants of nanoparticle clearance from the human body would be of tremendous benefit as this would permit more expeditous development of particles capable of renal clearance as well as permit the optimization of agents excretion via the hepatobiliary pathway. With this said, however, given the wide variation in particle material, size, and surface coating, it is likely that agent specific clearance studies will also be required.

Future Perspective

Harnessing the ability to synthesize molecules in a highly controlled manner, nanotechnology possesses great potential for the creation of designer agents with highly specific architechture. The application of nanotechnology to clinical medicine, referred to as nanomedicine, requires synthesizing nanoparticles with optimal *in vivo* characteristics. Research evaluating the relationship between nanoparticle characteristics and *in vivo* kinetics and excretion, as described in this review, is critical for the clinical implementation

of various nanoparticles. Utilization of this information will aid in the creation of biocompaticle and clinically feasible nanoparticles and will therefore contribute to the advancement of the field of nanomedicine.

Excutive Summary

- physiologic clearance of nano-sized reagents from the body
- behavior of nano-sized agents within the vascular system
- renal physiology and clearance of nano-sized agents
- hepatic physiology and clearance of nano-sized agents
- clearance of various nano-materials
- clearance of inorganic nano-materials
- clearance of biodegradeble nano-materials
- clearance of carbon-based nano-materials
- clearance of metal-based nano-crystals
- clearance of silica nano-particles

References

1. Hagens WI, Oomen AG, de Jong WH, Cassee FR, Sips AJ. What do we (need to) know about the kinetic properties of nanoparticles in the body? Regul Toxicol Pharmacol. Dec.2007 49:217–29. [PubMed: 17868963]
2. Ballou B, Ernst LA, Andreko S, Harper T, Fitzpatrick JA, Waggoner AS, Bruchez MP. Sentinel lymph node imaging using quantum dots in mouse tumor models. Bioconjug Chem. Mar-Apr.2007 18:389–96. [PubMed: 17263568]
3*. Choi HS, Liu W, Misra P, Tanaka E, Zimmer JP, Itty Ipe B, Bawendi MG, Frangioni JV. Renal clearance of quantum dots. Nat Biotechnol. Oct.2007 25:1165–70. [PubMed: 17891134] [An original work for the renal clearance of quantum dots nano-cristals with small sizes]
4. Csortos C, Kolosova I, Verin AD. Regulation of vascular endothelial cell barrier function and cytoskeleton structure by protein phosphatases of the PPP family. Am J Physiol Lung Cell Mol Physiol. Oct.2007 293:L843–54. [PubMed: 17693486]
5. Chapman AP, Antoniw P, Spitali M, West S, Stephens S, King DJ. Therapeutic antibody fragments with prolonged in vivo half-lives. Nat Biotechnol. Aug.1999 17:780–3. [PubMed: 10429243]
6. Goel A, Colcher D, Baranowska-Kortylewicz J, Augustine S, Booth BJ, Pavlinkova G, Batra SK. Genetically engineered tetravalent single-chain Fv of the pancarcinoma monoclonal antibody CC49: improved biodistribution and potential for therapeutic application. Cancer Res. Dec 15.2000 60:6964–71. [PubMed: 11156397]
7. Alazraki NP, Styblo T, Grant SF, Cohen C, Larsen T, Waldrop S, Aarsvold JN. Sentinel node staging of early breast cancer using lymphoscintigraphy and the intraoperative gamma detecting probe. Radiol Clin North Am. Sep.2001 39:947–56. viii. [PubMed: 11587063]
8*. Barrett T, Choyke PL, Kobayashi H. Imaging of the lymphatic system: new horizons. Contrast Media Mol Imaging. Nov.2006 1:230–45. [PubMed: 17191764] [Excellent review for lymphatic functions and imaging by the use of nano-sized imaging contrast agents]
9. Hamidi M, Azadi A, Rafiei P. Pharmacokinetic consequences of pegylation. Drug Deliv. Nov-Dec. 2006 13:399–409. [PubMed: 17002967]
10. Deen WM, Lazzara MJ, Myers BD. Structural determinants of glomerular permeability. Am J Physiol Renal Physiol. Oct.2001 281:F579–96. [PubMed: 11553505]
11. Ohlson M, Sorensson J, Haraldsson B. A gel-membrane model of glomerular charge and size selectivity in series. Am J Physiol Renal Physiol. Mar.2001 280:F396–405. [PubMed: 11181401]

12. Prescott LF, McAuslane JA, Freestone S. The concentration-dependent disposition and kinetics of inulin. Eur J Clin Pharmacol. 1991; 40:619–24. [PubMed: 1884745]

13. Kobayashi H, Yoo TM, Kim IS, Kim MK, Le N, Webber KO, Pastan I, Paik CH, Eckelman WC, Carrasquillo JA. L-lysine effectively blocks renal uptake of 125I- or 99mTc-labeled anti-Tac disulfide-stabilized Fv fragment. Cancer Res. Aug 15.1996 56:3788–95. [PubMed: 8706025]

14. Olmsted SS, Padgett JL, Yudin AI, Whaley KJ, Moench TR, Cone RA. Diffusion of macromolecules and virus-like particles in human cervical mucus. Biophys J. Oct.2001 81:1930–7. [PubMed: 11566767]

15. Wiener EC, Brechbiel MW, Brothers H, Magin RL, Gansow OA, Tomalia DA, Lauterbur PC. Dendrimer-based metal chelates: a new class of magnetic resonance imaging contrast agents. Magn Reson Med. Jan.1994 31:1–8. [PubMed: 8121264]

16. Kobayashi H, Brechbiel MW. Dendrimer-based nanosized MRI contrast agents. Curr Pharm Biotechnol. Dec.2004 5:539–49. [PubMed: 15579043]

17*. Kobayashi H, Brechbiel MW. Nano-sized MRI contrast agents with dendrimer cores. Adv Drug Deliv Rev. Dec 14.2005 57:2271–86. [PubMed: 16290152] [An exellent review for the kinetic and behavior of dendrimer-based nano-sized imaging agents of different sizes]

18*. Kobayashi H, Le N, Kim IS, Kim MK, Pie JE, Drumm D, Paik DS, Waldmann TA, Paik CH, Carrasquillo JA. The pharmacokinetic characteristics of glycolated humanized anti-Tac Fabs are determined by their isoelectric points. Cancer Res. Jan 15.1999 59:422–30. [PubMed: 9927057] [A work demonstrating that differently charged Fab molecules dractically altered the behavior in the kidney that led the completely different renal clearance properties]

19. Kuntz, E.; Kuntz, H-D. Hepatology : principles and practice : history, morphology, biochemistry, diagnostics, clinic, therapy. 2nd ed.. Vol. 3. Springer; Heidelberg: 2006. p. 19-24.

20*. Tomalia DA, Reyna LA, Svenson S. Dendrimers as multi-purpose nanodevices for oncology drug delivery and diagnostic imaging. Biochem Soc Trans. Feb.2007 35:61–7. [PubMed: 17233602] [An excellent review for the biomedical application of various dendrimers]

21. Bryant LH Jr. Brechbiel MW, Wu C, Bulte JW, Herynek V, Frank JA. Synthesis and relaxometry of high-generation (G = 5, 7, 9, and 10) PAMAM dendrimer-DOTA-gadolinium chelates. J Magn Reson Imaging. Feb.1999 9:348–52. [PubMed: 10077036]

22. Kobayashi H, Sato N, Hiraga A, Saga T, Nakamoto Y, Ueda H, Konishi J, Togashi K, Brechbiel MW. 3D-micro-MR angiography of mice using macromolecular MR contrast agents with polyamidoamine dendrimer core with reference to their pharmacokinetic properties. Magn Reson Med. Mar.2001 45:454–60. [PubMed: 11241704]

23. Malik N, Wiwattanapatapee R, Klopsch R, Lorenz K, Frey H, Weener JW, Meijer EW, Paulus W, Duncan R. Dendrimers: relationship between structure and biocompatibility in vitro, and preliminary studies on the biodistribution of 125I-labelled polyamidoamine dendrimers in vivo. J Control Release. Mar 1.2000 65:133–48. [PubMed: 10699277]

24. Kobayashi H, Wu C, Kim MK, Paik CH, Carrasquillo JA, Brechbiel MW. Evaluation of the in vivo biodistribution of indium-111 and yttrium-88 labeled dendrimer-1B4M-DTPA and its conjugation with anti-Tac monoclonal antibody. Bioconjug Chem. Jan-Feb.1999 10:103–11. [PubMed: 9893971]

25. Sato N, Kobayashi H, Hiraga A, Saga T, Togashi K, Konishi J, Brechbiel MW. Pharmacokinetics and enhancement patterns of macromolecular MR contrast agents with various sizes of polyamidoamine dendrimer cores. Magn Reson Med. Dec.2001 46:1169–73. [PubMed: 11746584]

26. Kobayashi H, Jo SK, Kawamoto S, Yasuda H, Hu X, Knopp MV, Brechbiel MW, Choyke PL, Star RA. Polyamine dendrimer-based MRI contrast agents for functional kidney imaging to diagnose acute renal failure. J Magn Reson Imaging. Sep.2004 20:512–8. [PubMed: 15332261]

27. Kobayashi H, Kawamoto S, Jo SK, Bryant HL Jr. Brechbiel MW, Star RA. Macromolecular MRI contrast agents with small dendrimers: pharmacokinetic differences between sizes and cores. Bioconjug Chem. Mar-Apr.2003 14:388–94. [PubMed: 12643749]

28. Mohs AM, Lu ZR. Gadolinium(III)-based blood-pool contrast agents for magnetic resonance imaging: status and clinical potential. Expert Opin Drug Deliv. Mar.2007 4:149–64. [PubMed: 17335412]

29. Dong Q, Hurst DR, Weinmann HJ, Chenevert TL, Londy FJ, Prince MR. Magnetic resonance angiography with gadomer-17. An animal study original investigation. Invest Radiol. Sep.1998 33:699–708. [PubMed: 9766055]
30. Feng Y, Zong Y, Ke T, Jeong EK, Parker DL, Lu ZR. Pharmacokinetics, biodistribution and contrast enhanced MR blood pool imaging of Gd-DTPA cystine copolymers and Gd-DTPA cystine diethyl ester copolymers in a rat model. Pharm Res. Aug.2006 23:1736–42. [PubMed: 16850267]
31. Zong Y, Wang X, Goodrich KC, Mohs AM, Parker DL, Lu ZR. Contrast-enhanced MRI with new biodegradable macromolecular Gd(III) complexes in tumor-bearing mice. Magn Reson Med. Apr. 2005 53:835–42. [PubMed: 15799038]
32*. Lu ZR, Parker DL, Goodrich KC, Wang X, Dalle JG, Buswell HR. Extracellular biodegradable macromolecular gadolinium(III) complexes for MRI. Magn Reson Med. Jan.2004 51:27–34. [PubMed: 14705042] [An important conceptional work for the biodegradable nano-molecules]
33. Rao J, Dragulescu-Andrasi A, Yao H. Fluorescence imaging in vivo: recent advances. Curr Opin Biotechnol. Feb.2007 18:17–25. [PubMed: 17234399]
34. Yang RS, Chang LW, Wu JP, Tsai MH, Wang HJ, Kuo YC, Yeh TK, Yang CS, Lin P. Persistent tissue kinetics and redistribution of nanoparticles, quantum dot 705, in mice: ICP-MS quantitative assessment. Environ Health Perspect. Sep.2007 115:1339–43. [PubMed: 17805425]
35. Hardman R. A toxicologic review of quantum dots: toxicity depends on physicochemical and environmental factors. Environ Health Perspect. Feb.2006 114:165–72. [PubMed: 16451849]
36. Ballou B, Lagerholm BC, Ernst LA, Bruchez MP, Waggoner AS. Noninvasive imaging of quantum dots in mice. Bioconjug Chem. Jan-Feb.2004 15:79–86. [PubMed: 14733586]
37. Fischer HC, Liu L, Pang KS, Chan WCW. Pharmacokinetics of nanoscale quantum dots: In vivo distribution, sequestration, and clearance in the rat. Adv Funct Mater. Jul.2006 16:1299–305.
38. Schipper ML, Cheng Z, Lee SW, Bentolila LA, Iyer G, Rao J, Chen X, Wu AM, Weiss S, Gambhir SS. MicroPET-based biodistribution of quantum dots in living mice. J of Nucl Med. Sep.2007 48:1211–18.
39. Chan, WCW. Bio-Applications of Nanoparticles. Landes Bioscience; Austin, Texas: 2007.
40. Sitharaman B, Tran LA, Pham QP, Bolskar RD, Muthupillai R, Flamm SD, Mikos AG, Wilson LJ. Gadofullerenes as nanoscale magnetic labels for cellular MRI. Contrast Media Mol Imaging. May. 2007 2:139–46. [PubMed: 17583898]
41. Kato H, Kanazawa Y, Okumura M, Taninaka A, Yokawa T, Shinohara H. Lanthanoid endohedral metallofullerenols for MRI contrast agents. J Am Chem Soc. Apr 9.2003 125:4391–7. [PubMed: 12670265]
42. Bolskar RD, Benedetto AF, Husebo LO, Price RE, Jackson EF, Wallace S, Wilson LJ, Alford JM. First soluble M@C60 derivatives provide enhanced access to metallofullerenes and permit in vivo evaluation of Gd@C60[C(COOH)2]10 as a MRI contrast agent. J Am Chem Soc. May 7.2003 125:5471–8. [PubMed: 12720461]
43. Fatouros PP, Corwin FD, Chen ZJ, Broaddus WC, Tatum JL, Kettenmann B, Ge Z, Gibson HW, Russ JL, et al. In vitro and in vivo imaging studies of a new endohedral metallofullerene nanoparticle. Radiology. Sep.2006 240:756–64. [PubMed: 16837672]
44. Toth E, Bolskar RD, Borel A, Gonzalez G, Helm L, Merbach AE, Sitharaman B, Wilson LJ. Water-soluble gadofullerenes: toward high-relaxivity, pH-responsive MRI contrast agents. J Am Chem Soc. Jan 19.2005 127:799–805. [PubMed: 15643906]
45. Cagle DW, Kennel SJ, Mirzadeh S, Alford JM, Wilson LJ. In vivo studies of fullerene-based materials using endohedral metallofullerene radiotracers. Proc Natl Acad Sci U S A. Apr 27.1999 96:5182–7. [PubMed: 10220440]
46. Cherukuri P, Gannon CJ, Leeuw TK, Schmidt HK, Smalley RE, Curley SA, Weisman RB. Mammalian pharmacokinetics of carbon nanotubes using intrinsic near-infrared fluorescence. Proc Natl Acad Sci U S A. Dec 12.2006 103:18882–6. [PubMed: 17135351]
47. Singh R, Pantarotto D, Lacerda L, Pastorin G, Klumpp C, Prato M, Bianco A, Kostarelos K. Tissue biodistribution and blood clearance rates of intravenously administered carbon nanotube radiotracers. Proc Natl Acad Sci U S A. Feb 28.2006 103:3357–62. [PubMed: 16492781]

48. Liu Z, Davis C, Cai W, He L, Chen X, Dai H. Circulation and long-term fate of functionalized, biocompatible single-walled carbon nanotubes in mice probed by Raman spectroscopy. Proc Natl Acad Sci U S A. Feb 5.2008 105:1410–5. [PubMed: 18230737]
49. Szoka F Jr. Papahadjopoulos D. Comparative properties and methods of preparation of lipid vesicles (liposomes). Annu Rev Biophys Bioeng. 1980; 9:467–508. [PubMed: 6994593]
50. Jiang W, Kim BY, Rutka JT, Chan WC. Advances and challenges of nanotechnology-based drug delivery systems. Expert Opin Drug Deliv. Nov.2007 4:621–33. [PubMed: 17970665]
51. Ishida T, Harashima H, Kiwada H. Liposome clearance. Bioscience Reports. 2002; 22:197–224. [PubMed: 12428901]
52. Chonn A, Semple SC, Cullis PR. Association of blood proteins with large unilamellar liposomes in vivo. Relation to circulation lifetimes. J Biol Chem. Sep 15.1992 267:18759–65. [PubMed: 1527006]
53. Chonn A, Cullis PR, Devine DV. The role of surface charge in the activation of the classical and alternative pathways of complement by liposomes. J Immunol. Jun 15.1991 146:4234–41. [PubMed: 2040798]
54. Funato K, Yoda R, Kiwada H. Contribution of complement system on destabilization of liposomes composed of hydrogenated egg phosphatidylcholine in rat fresh plasma. Biochim Biophys Acta. Jan 31.1992 1103:198–204. [PubMed: 1543704]
55. Senior JH. Fate and behavior of liposomes in vivo: a review of controlling factors. Crit Rev Ther Drug Carrier Syst. 1987; 3:123–93. [PubMed: 3542245]
56. Harashima H, Sakata K, Funato K, Kiwada H. Enhanced hepatic uptake of liposomes through complement activation depending on the size of liposomes. Pharm Res. Mar.1994 11:402–6. [PubMed: 8008707]
57. Harashima H, Huong TM, Ishida T, Manabe Y, Matsuo H, Kiwada H. Synergistic effect between size and cholesterol content in the enhanced hepatic uptake clearance of liposomes through complement activation in rats. Pharm Res. Nov.1996 13:1704–9. [PubMed: 8956338]
58. Zheng J, Liu J, Dunne M, Jaffray DA, Allen C. In vivo performance of a liposomal vascular contrast agent for CT and MR-based image guidance applications. Pharm Res. Jun.2007 24:1193–201. [PubMed: 17373581]
59. McLachlan SJ, Eaton S, De Simone DN. Pharmacokinetic behavior of gadoteridol injection. Invest Radiol. Aug; 1992 27(Suppl 1):S12–5. [PubMed: 1506147]
60. Arvidsson A, Hedman A. Plasma and renal clearance of iohexol--a study on the reproducibility of a method for the glomerular filtration rate. Scand J Clin Lab Invest. Nov.1990 50:757–61. [PubMed: 2293336]
61. Hainfeld JF, Slatkin DN, Focella TM, Smilowitz HM. Gold nanoparticles: a new X-ray contrast agent. Br J Radiol. Mar.2006 79:248–53. [PubMed: 16498039]
62. Hirsch LR, Gobin AM, Lowery AR, Tam F, Drezek RA, Halas NJ, West JL. Metal nanoshells. Ann Biomed Eng. Jan.2006 34:15–22. [PubMed: 16528617]
63. Zhou HS, Honma II, Komiyama H, Haus JW. Controlled synthesis and quantum-size effect in gold-coated nanoparticles. Phys Rev B Condens Matter. Oct 15.1994 50:12052–6. [PubMed: 9975346]
64. Oldenburg SA, R.D. Westcott S, Halas NJ. Nanoengineering of Optical Resonances. Chemical Physics Letters. 1998:288.
65. De Jong WH, Hagens WI, Krystek P, Burger MC, Sips AJ, Geertsma RE. Particle size-dependent organ distribution of gold nanoparticles after intravenous administration. Biomaterials. Apr.2008 29:1912–9. [PubMed: 18242692]
66. Chen J, Saeki F, Wiley BJ, Cang H, Cobb MJ, Li ZY, Au L, Zhang H, Kimmey MB, et al. Gold nanocages: bioconjugation and their potential use as optical imaging contrast agents. Nano Lett. Mar.2005 5:473–7. [PubMed: 15755097]
67. Kattumuri V, Katti K, Bhaskaran S, Boote EJ, Casteel SW, Fent GM, Robertson DJ, Chandrasekhar M, Kannan R, Katti KV. Gum arabic as a phytochemical construct for the stabilization of gold nanoparticles: in vivo pharmacokinetics and X-ray-contrast-imaging studies. Small. Feb.2007 3:333–41. [PubMed: 17262759]

68. Bonnemain B. Superparamagnetic agents in magnetic resonance imaging: physicochemical characteristics and clinical applications. A review. J Drug Target. 1998; 6:167–74. [PubMed: 9888302]
69. Corot C, Robert P, Idee JM, Port M. Recent advances in iron oxide nanocrystal technology for medical imaging. Adv Drug Deliv Rev. Dec 1.2006 58:1471–504. [PubMed: 17116343]
70. Benderbous S, Corot C, Jacobs P, Bonnemain B. Superparamagnetic agents: physicochemical characteristics and preclinical imaging evaluation. Acad Radiol. Aug; 1996 3(Suppl 2):S292–4. [PubMed: 8796583]
71. Chouly C, Pouliquen D, Lucet I, Jeune JJ, Jallet P. Development of superparamagnetic nanoparticles for MRI: effect of particle size, charge and surface nature on biodistribution. J Microencapsul. May-Jun.1996 13:245–55. [PubMed: 8860681]
72. Jain TK, Reddy MK, Morales MA, Leslie-Pelecky DL, Labhasetwar V. Biodistribution, Clearance, and Biocompatibility of Iron Oxide Magnetic Nanoparticles in Rats. Mol Pharm. Apr 7.2008 5:316–27. [PubMed: 18217714]
73. Briley-Saebo K, Bjornerud A, Grant D, Ahlstrom H, Berg T, Kindberg GM. Hepatic cellular distribution and degradation of iron oxide nanoparticles following single intravenous injection in rats: implications for magnetic resonance imaging. Cell & Tissue Research. 2004; 316:315–23. [PubMed: 15103550]
74. Bourrinet P, Bengele HH, Bonnemain B, Dencausse A, Idee JM, Jacobs PM, Lewis JM. Preclinical safety and pharmacokinetic profile of ferumoxtran-10, an ultrasmall superparamagnetic iron oxide magnetic resonance contrast agent. Invest Radiol. Mar.2006 41:313–24. [PubMed: 16481915]
75. Wisse E, Doucet D, Van Bossuyt H. A transmission electron microscopic study on the uptake of AMI-25 by sinusoidal liver cells. Cells of the hepatic sinusoid. 1991; 3:534039.
76. Yao G, Wang L, Wu Y, Smith J, Xu J, Zhao W, Lee E, Tan W. FloDots: luminescent nanoparticles. Anal Bioanal Chem. Jun.2006 385:518–24. [PubMed: 16715275]
77. Taylor KM, Kim JS, Rieter WJ, An H, Lin W. Mesoporous silica nanospheres as highly efficient MRI contrast agents. J Am Chem Soc. Feb 20.2008 130:2154–5. [PubMed: 18217764]

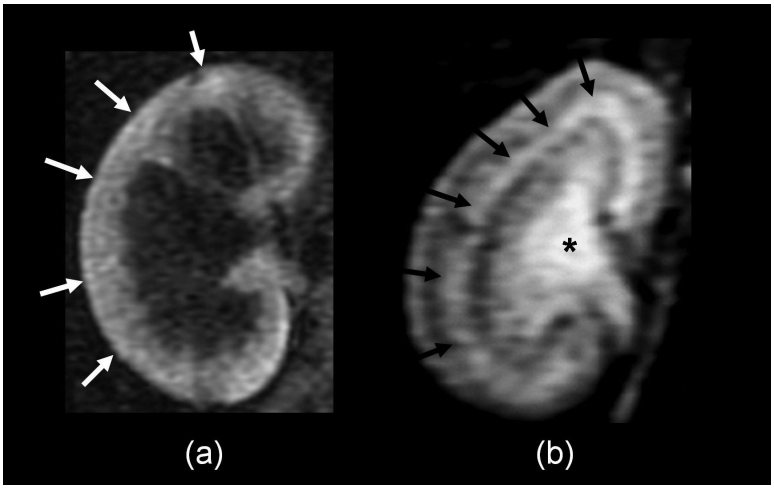

Figure 1.
2D-T1 weighted MR images of kidneys with acute tubular dysfunction (a) and normal function (b) are shown. Glomerular filtration (white arrows) is shown in the kidney when the tubular function is completely impaired (a) and tubular concentration function (black arrows) and urinary excretion (*) are shown in the normal functioning kidney (b).

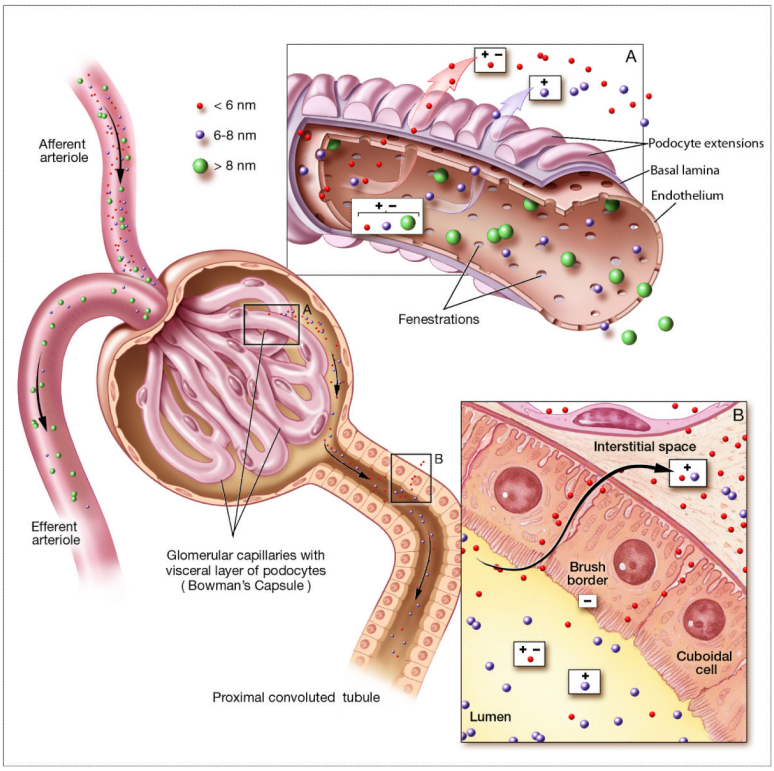

Figure 2.

Renal handling of nanoparticles of different sizes and charges. Circulating nanoparticles enter the glomerular capillary bed via the afferent arteriole. A) The glomerular capillary wall is composed of three layers: fenestrated endothelium; the highly negatively charged glomerular basement membrane (GBM); and podocyte extensions of glomerular epithelial cells. Glomerular filtrate flows through the fenestrate, across the GBM, and through filtration slits formed by spaces between podocyte extensions. The primary size barrier is the filtration slit, which has a physiologic pore size of 4.5-5 nm. Nanoparticles < 6 nm (red) are small enough to be freely filtered, irrespectively of molecular charge. However, glomerular filtration of particles between 6-8 nm (purple) is dependent on charge interactions between the intermediate sized particles and the negative charges of the GBM. Therefore, positively particles are more readily filtered than equally sized negatively charged particles. Due to size limitations, particles > 8 nm do not undergo glomerular filtration. After glomerular filtration, filtered nanoparticles enter the proximal tubule. B) Within the proximal tubule, nanoparticles may be resorbed from the luminal space. Since the brush border of the proximal tubule epithelial cells is negatively charged, positively charged particles are more readily resorbed than comparable negatively charged particles.

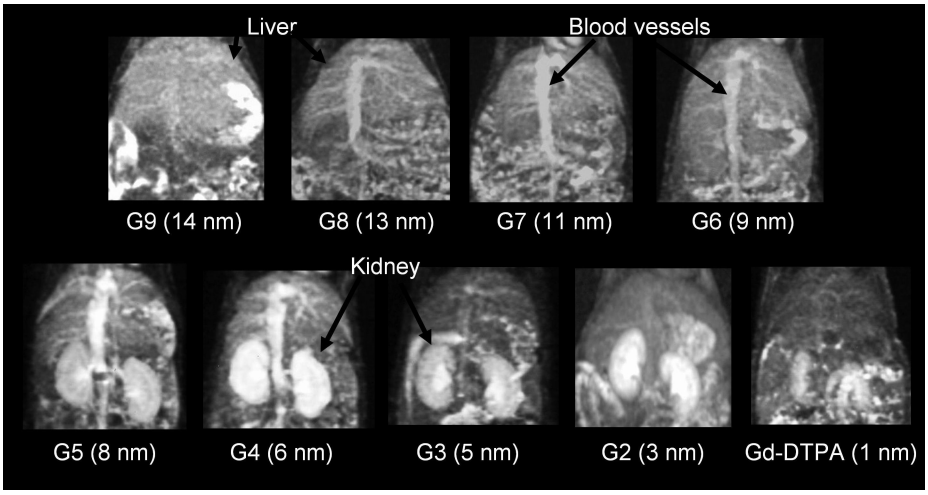

Figure 3.

3D-maximum intensity projection display of T1-weighted MR images of the abdomen at 15 min post-injection for G9, G8, G7, and G6 and at 3 min after injection for G5, G4, G3, G2, and DTPA are shown. Kidneys are shown with agents of G5 (8 nm in diameter) or smaller. Blood pool is clearly depicted G5 (8 nm) and G4 (5 nm) at 3 min post-injection because of partial and slow glomerular filtration. Kidneys are not shown with agents G6 (9 nm in diameter) or larger even at 15 min post-injection. Intensities in the liver increase as the agent sizes increase.

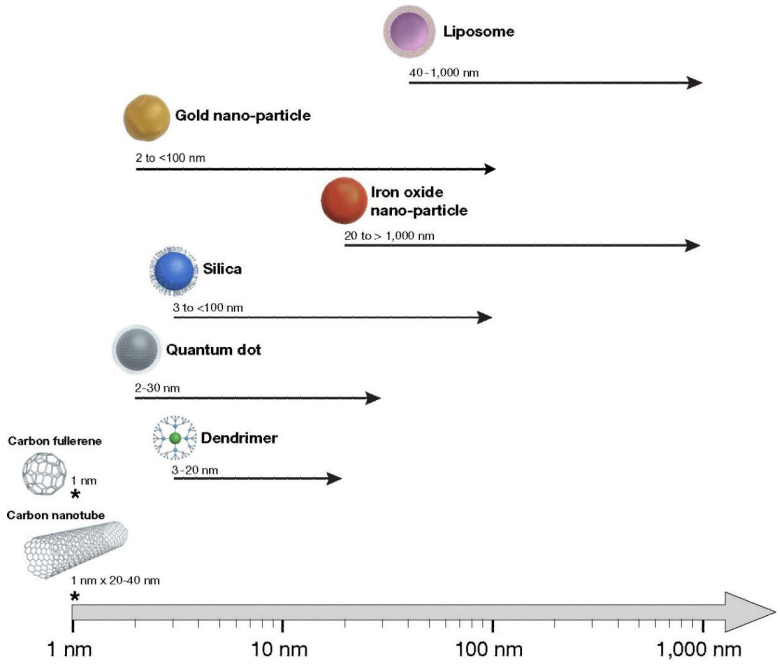

Figure 4.

Comparison of sizes of various nanoparticles. Chemical composition and size range are defining features for nanoparticles. Both characteristics are important determinants of nanoparticle *in vivo* behavior and clearance properties.